ACS APPLIED MATERIALS & INTERFACES

Research Article

www.acsami.org

Biomimetic Mushroom-Shaped Microfibers for Dry Adhesives by Electrically Induced Polymer Deformation

Hong Hu,[†] Hongmiao Tian,[†] Xiangming Li,[†] Jinyou Shao,*[,†] Yucheng Ding,[†] Hongzhong Liu,[†] and Ningli An[‡]

[†]Micro- and Nano-manufacturing Research Center, State Key Laboratory for Manufacturing Systems Engineering, Xi'an Jiaotong University, Xi'an, Shaanxi 710049, China

[‡]College of Printing and Packaging Engineering, Xi'an University of Technology, Xi'an, Shaanxi 710048, China

ABSTRACT: The studies on bioinspired dry adhesion have demonstrated the biomimetic importance of a surface arrayed with mushroom-shaped microfibers among other artificially textured surfaces. The generation of a mushroom-shaped microfiber array with a high aspect ratio and a large tip diameter remains to be investigated. In this paper we report a three-step process for producing mushroom-shaped microfibers with a well-controlled aspect ratio and tip diameter. First, a polymer film coated on an electrically conductive substrate is prestructured into a low-aspect-ratio micropillar array by hot embossing. In the second step, an electrical voltage is applied to an electrode pair composed of the substrate and another conductive planar plate, sandwiching an air clearance. The Maxwell force induced on the air−polymer interface by the electric field electrohydrodynamically pulls the preformed micropillars upward to contact the upper electrode. Finally, the micropillars spread transversely on this electrode due to the electrowetting effect, forming the mushroom tip. In this paper we have demonstrated a polymer surface arrayed with mushroom-shaped microfibers with a large tip diameter (3 times the shaft diameter) and a large aspect ratio (above 10) and provided the testing results for dry adhesion.

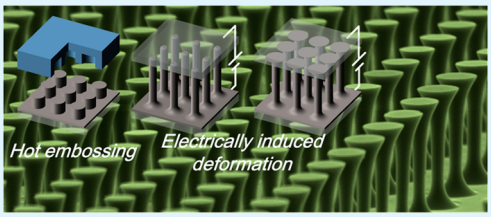

KEYWORDS: *biomimetics, microfiber arrays, dry adhesive, electrohydrodynamics*

1. INTRODUCTION

Creatures that exhibit extraordinary abilities in daily activities employ a variety of strategies to achieve them. For example, geckos have evolved the ability to adhere to almost any surface: smooth or rough, hydrophobic or hydrophilic, and wall or ceiling.[1,2] This so-called "dry adhesion" ability has been considered to be due to their unique toe pads, which feature an extraordinary hierarchy of microstructure in the form of an array of millions of high-aspect-ratio fibers.[3−7] Inspired by this biofunctionality, fiber tips engineered with various geometries such as pillars with a flat, spherical, concave, or mushroom-shaped top have also demonstrated significantly different behavior in dry adhesion.[6−12] Biomimetically prominent among these geometries is the mushroom-shaped tip array of a high aspect ratio, which has been proved to be desirable for this surface functionality due to its obvious contribution to enhancing the van der Waals interactions.[8,9,11−13]

Therefore, the fabrication of this mushroom-shaped microfiber array has attracted much interest, resulting in numerous new techniques. The replica molding technique, in which usually polymer materials such as poly(dimethylsiloxane) (PDMS) or polyurethane are cast into a silicon mold (or master) structured by photolithography or etching, is the most often used approach.[11,12,14−19] This process starts from a pivotal fabrication of a silicon master arrayed with undercut microholes by inserting an etch-stop layer of silicon dioxide and carefully conducting deep and isotropic reactive ion etching on a poly-Si substrate. Subsequently, the mushroom-shaped microfibers can be achieved through a demolding, which is usually conducted by carefully peeling the cured polymer out of the master[15−17] or sacrificing the master via a selective chemical etching.[18,19] These replica molding techniques are mature and highly productive and hence are widely employed by many research groups for fabricating the bioinspired mushroom-shaped adhesives. However, as pointed out in this research, these techniques may be faced with a challenge in the demolding by the peeling-off method, which can often lead to distortion and damage to the replicated structures, especially when the microfibers with a large tip ending diameter or a high aspect ratio are required,[16,17] while the demolding by sacrificing the master would be undesirable for process economy.[20] An approach for avoiding this demolding problem would be a two-step sequential process, which generates first the lower supporting pillars and then the upper tip endings. For example, mechanical pressing on partially cured micro- or nanopillars generated by molding of a UV-curable resin has been reported as a simple technique for fabricating micro- or nanofibers with controllable mushroom-shaped tip endings.[21] Since this approach is based on a modification of the preformed pillars by mechanical pressing, it can risk a structural loss or crushing on the prestructured yet incompletely cured polymer, especially when a relatively large pressing force has to be used for forming

Received: June 3, 2014
Accepted: August 7, 2014
Published: August 7, 2014

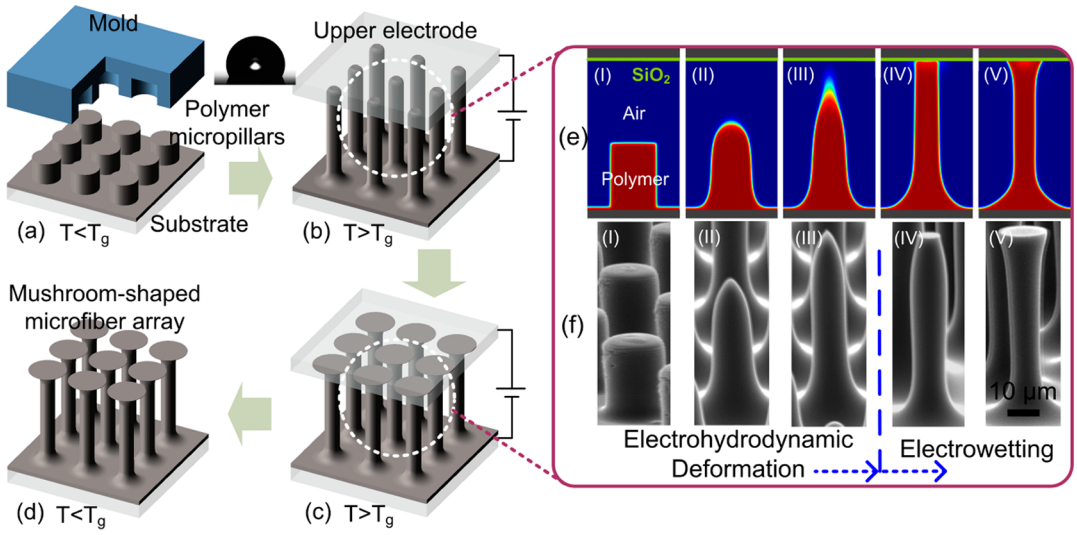

Figure 1. Illustration of the three-step process for fabricating a bioinspired mushroom-shaped microfiber array with a high aspect ratio. (a) The first step entails hot embossing for prestructuring the polymer to a micropillar array with a low aspect ratio on a conductive substrate. (b) The second step involves application of a voltage to electrohydrodynamically pull the micropillars upward into contact with the upper electrode while the polymer is heated to its glass transition temperature (T_g) for liquefaction. The inset shows the wet experiment demonstrating the low surface energy of the FAS-treated upper electrode. (c) The third step is the transverse spreading of the micropillar tip on the upper electrode coated with dielectric SiO_2 by electrowetting. (d) The upper electrode is then removed. Insets (e) and (f) show the evolutions of the prestructured and liquefied polymer induced by an external electric field and obtained numerically and experimentally.

a large-diameter tip ending on the high-aspect-ratio pillars. Similarly, mushroom-shaped tips have also been formed by dipping the preformed and fully cured polymer pillars into a liquid-state prepolymer and then pressing them onto a planar plate with a constant load, followed by the curing of the superimposed prepolymer at room temperature.[6,22] This method offers an improved approach to prepare mushroom-shaped microfibers, while it can also face a challenge in controlling the tip ending diameter, which depends mainly on the inherent wettability of the prepolymer on the plate.

In this paper we report a facile approach for fabricating the bioinspired mushroom-shaped microfiber array with a well-controlled aspect ratio and tip ending diameter, which, as a three-step process, is a combination of hot embossing, electrically induced deformation of the polymer, and electrowetting. First, a polymer film coated on an electrically conductive substrate is prestructured into a low-aspect-ratio micropillar array by hot embossing. Confined by the mold geometry and process capacity, the preformed micropillar array has a nearly flat or spherical tip. In the second step, an electrical voltage is applied to an electrode pair (or a capacitor) composed of the substrate with the preformed micropillar array and another conductive planar plate, which is placed parallel with the substrate at an air clearance above the initial micropillars (with the gap between the upper plate and substrate being the capacitor clearance). Because the top of the preformed micropillars has a smaller distance to the upper electrode than the bottom does, a spatially nonuniform electric field is generated on the air/polymer interface due to a modulation by the micropillar array. The Maxwell force induced on the polymer by such an electric field electrohydrodynamically pulls the preformed micropillars upward to contact the upper electrode, so as to extend the micropillars to an increased aspect ratio on the condition that the polymer is thermally maintained above its glass-state temperature.[23] Importantly, in the third step, after the micropillars contact the upper electrode, the micropillars spread transversely on this electrode surface due to the electrowetting effect, generating a microfiber array with a high aspect ratio and a large-diameter tip (or cap). Clearly, such a mushroom-shaped microfiber array features an aspect ratio exactly defined by the air clearance of the upper electrode above the initially preformed shallow micropillars and a tip diameter well controlled by the electrowetting of the thermally flowing polymer on the upper electrode. To enhance the electrowetting effect, a dielectric layer is coated on the upper electrode and then treated chemically for low surface energy, leading to an "electrowetting effect on dielectric" (or EWOD[24]) and still an easy removal of the upper electrode. Notably, the electrohydrodynamic-based technique we propose here enables a relatively easier demolding process, which is essentially required for the fabrication of mushroom-shaped microfibers with a high aspect ratio and large tip diameter, and it is applicable for almost any thermoplastic polymer, allowing for the use of a mechanically strong or hard polymer, which is critical for maintaining a proper mechanical integrity for the long running of such a biomimetically structured surface.[20,22,25]

2. EXPERIMENTAL DETAILS

2.1. Summary of the Process Steps. Figure 1 shows the process flow of the proposed approach for fabricating biomimetic mushroom-shaped microfibrillar adhesives. First, a poly(methyl methacrylate) (PMMA)-coated conductive substrate (functioning as the lower electrode) was prepared for hot embossing, during which a microhole-arrayed silicon template, having a patterned area of 1 × 1 cm^2, was pressed against the PMMA-coated substrate using a constant pressure of roughly 50 kPa, and the assembly was maintained thermally at ~140 °C for ~15 min and then cooled for roughly 20 min. For an easy demolding, hot embossing can be performed to lead to a shallow PMMA micropillar array by using a template arrayed with microholes of low aspect ratio (smaller than 1.0 in this experiment). Next, another conductive planar plate (made of a deeply and strongly doped silicon wafer with an electrical resistivity of ~0.005–0.015 Ω cm in this experiment) was employed as the upper electrode, which was mounted above the preformed micropillars with an air clearance

made by dielectric spacers and combined with the lower substrate into a parallel electrode pair sandwiching the air clearance and the preformed micropillars. Importantly, a dielectric SiO_2 film with a thickness of ~1.2 μm was coated on the surface of this electrode by a thermal oxidation process. The reason for the necessity of the dielectric SiO_2 layer and its effects on the electric field distribution and the structural morphology of the final microfiber array will be discussed in detail later. The upper electrode coated with SiO_2 was then treated in a 1.0 wt % ethanol solution of (heptadecafluorodecyl)-trimethoxysilane (abbreviated FAS, $CF_3(CF_2)_7CH_2CH_2Si(OCH_3)_3$) for 5 h and subsequently baked at 150 °C for 10 h to produce an antiadhesion layer, which is required for an easy separation of the microfiber array from the upper electrode in the final step. As a result, the contact angle of a water droplet on the FAS-treated upper electrode was ~115°, as shown in the inset of Figure 1. The assembly was then thermally maintained above the glass transition temperature of PMMA again for liquefaction, while an electric voltage was applied to the electrode pair (Figure 1b). Notably, a relatively high temperature of ~170 °C, much closer to the melting point of PMMA, could be better for a high-efficiency electrically induced deformation process, as the thermoplastic polymer was much easier to flow (low dynamic viscosity coefficient) under such a temperature. The Maxwell force induced by the electric field pulls the micropillars upward to contact the upper plate, resulting in an extended aspect ratio for the micropillars. Then the sustaining voltage further causes the micropillars in contact with the upper plate to spread transversely on the upper electrode (Figure 1c) due to the electrowetting effect. In this experiment, the electrically driven polymer deformation as a whole took time, ranging from 3 to 5 h. After the assembly was cooled to room temperature, a mechanical removal of the upper electrode left a microfiber array on the substrate, with a large aspect ratio and a flat tip with a large diameter (Figure 1d).

For a better understanding of the electrically induced polymer deformation process, Figure 1 also shows the evolving deformation of a preformed and thermally liquefied polymer micropillar between the electrode pair, which was obtained from a numerical simulation based on an electrohydrodynamic and phase-field formulation (Figure 1e)[26,27] and from the corresponding experiment (Figure 1f). Clearly, the electrodynamic force not only pulled the prestructured and liquefied polymer upward to contact the upper electrode (as shown in parts e(I–III) and f(I–III) of Figure 1) to extend its aspect ratio, but also pushed the polymer to wet the solid dielectric layer (SiO_2) coated on the upper electrode so that the top of the polymer spread transversely on the dielectric layer (as shown in parts e(IV), e(V), fI(V), and f(V) of Figure 1), increasing the diameter of the tip of the polymer pillar. Therefore, the electrically induced generation of the microfibers can be divided into two electrodynamic phases of the polymer, namely, electrohydrodynamic deformation and EWOD[24,28,29].

2.2. Materials and Equipment. PMMA (MW 15K) was purchased from Sigma-Aldrich Inc. The Young modulus of the cured PMMA used in this experiment was about 1–2 GPa, as specified by the material vendor. The effective modulus of the structures was about 0.8–1.6 MPa. The obvious reduction was due to the replacement of the solid PMMA block with an array of mushroom-shaped microfibers.[30,31] The conductive substrate was made of a slide glass on which an indium tin oxide (ITO) layer with a thickness of 200 nm was sputtered using a Denton Vacuum Explorer 14 sputtering system. A 10 wt % solution of PMMA in toluene was blade-cast on the conductive substrate to produce a ~30 μm thick film, which was baked at 120 °C for 5 min to remove the solvent by evaporation. The mold for hot embossing was a silicon master fabricated by conventional photolithography and an inductively coupled plasma (ICP) etching process in an ICP chemical vapor deposition (CVD) chamber (Oxford ICP-180). The upper electrode was a deeply and strongly doped silicon wafer, which was coated with a thermally grown SiO_2 layer. The dc voltage was applied using an amplifier/controller (TREK 610E HV). The scanning electron microscope (SEM) images were recorded using a Hitachi S-3000N SEM instrument.

3. RESULTS AND DISCUSSION

3.1. Electrically Induced Deformation for High-Aspect-Ratio Microfibers. Because the electrodynamic behavior is highly dependent on the electric field intensity, the capacitor clearance in the electrode pair and the applied voltage are the two critical process variables for the successful formation of the mushroom-shaped microfibers for a certain initial height of the hot-embossed micropillar array. In short, the capacitor clearance defines the final height or aspect ratio of the microfibers, while the applied voltage determines whether the electrodynamic force is sufficient to drive the polymer upward by overcoming the surface tension and viscous resistance of the polymer for a certain initial height of the micropillars.

To characterize the electrohydrodynamic process of the prestructured polymer and find a suitable applied voltage for a certain capacitor clearance, one can analyze the early-stage kinetics of a single pillar using the well-understood physical principles underlying the destabilization of thin films by electric fields.[32−34] In this theory, the continuous polymer film surface is represented as a combination of a series of waves, each corresponding to a growth coefficient due to the film fluctuation and external electric field. The dispersion relationship for the wave spectrum can be expressed as follows:[33,34]

$$\omega = -h^3[(\partial p_e/\partial h)q^2 + \sigma q^4]/3\eta \quad (1)$$

where q is the wavenumber, σ is the surface tension coefficient, η is the dynamic viscosity coefficient of the liquefied polymer, h is the film thickness, p_e is the electrohydrodynamic pressure, and ω is the growth coefficient, characterizing the early-stage kinetics of a certain wavenumber. In the proposed approach, the flat film was replaced by a micropillar array. This difference generated two main changes in the linear stability: (1) the micropillar array on a large-area film can be regarded as an artificially amplified fluctuation with an explicit wavelength (equal to the pitch of the micropillars, 30 μm in this experiment), and its growth coefficient determines whether the micropillars grow continuously upward in the periodicity of the initial hot-embossed structure; (2) the electrohydrodynamic pressure on the polymer surface along the horizontal direction is no longer constant, and the effective value for the spatially alternative electrohydrodynamic pressure, p_e, is equal to the difference between the electrohydrodynamic pressures at the top and at the bottom of the initial hot-embossed micropillars,[23,35] i.e.

$$p_e = p_{e,max} - p_{e,min} = -\frac{1}{2}\varepsilon_0\varepsilon_p(\varepsilon_p - 1)(E_{max}^2 - E_{min}^2) \quad (2)$$

where $p_{e,max}$ and $p_{e,min}$ are the electrohydrodynamic pressures on the free surface corresponding to the top and bottom of the initial micropillars, respectively, ε_p and ε_0 are the permittivities of the polymer and vacuum, respectively, and E_{max} and E_{min} are the maximum and minimum electric intensities, respectively. Thus, the dispersion relationship (eq 1) can be modified and normalized as follows:

$$\left(\omega\frac{3\eta}{\sigma h^3\alpha^4}\right) = \left(\frac{q}{\alpha}\right)^2 - \left(\frac{q}{\alpha}\right)^4 \quad (3)$$

where $\alpha = (\varepsilon_0\varepsilon_p(\varepsilon_p - 1)^2(E_{max}^3 - E_{min}^3)/\sigma U)^{1/2}$ and U represents the applied voltage across the electrode pair. As a general assumption in the electrohydrodynamic (EHD)-based

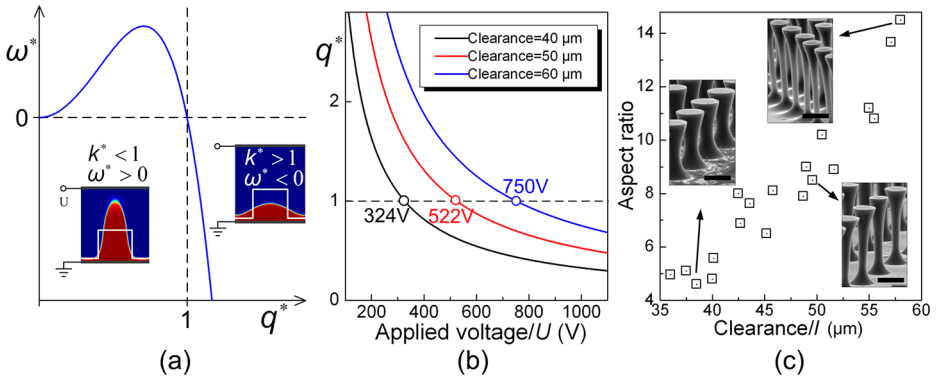

Figure 2. Characterization of the electrically induced pillar growth: (a) mapping relationship of the dimensionless variables ω^* (growth coefficient) and q^* (wavenumber); (b) relationship between q^* and applied voltage; (c) evolution of the aspect ratio with capacitor clearance. The scale bars in the insets are 15 μm.

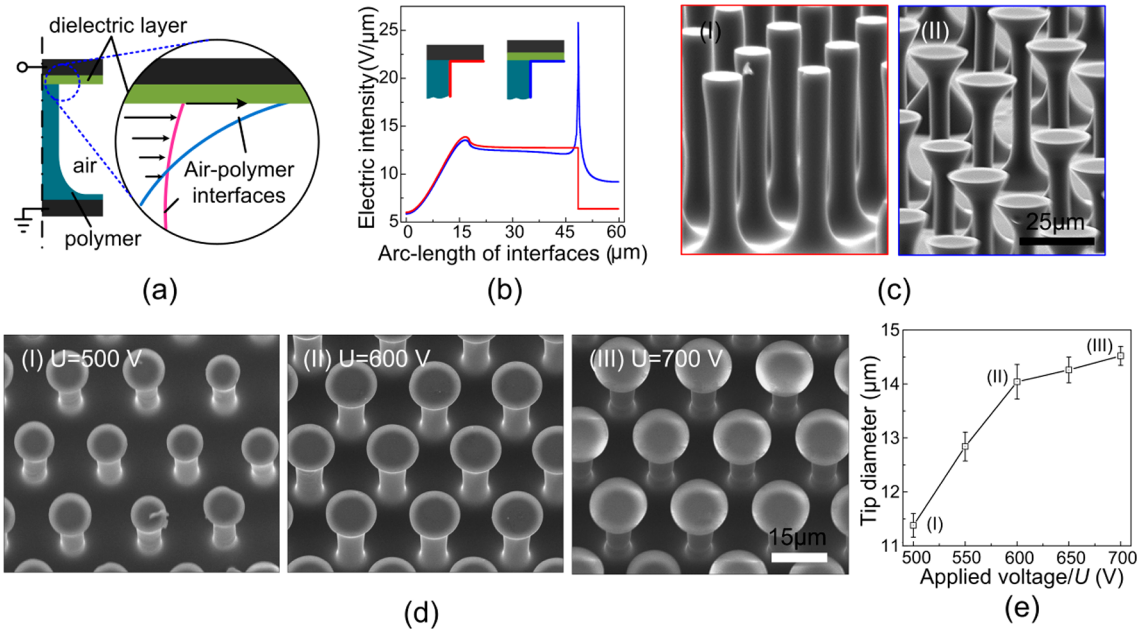

Figure 3. Electrowetting of thermally liquefied polymer for the generation of transversely extended pillar tips: (a) EWOD for enhanced electrowetting (with the arrows representing the horizontal component of the Maxwell force); (b) electric field distribution determined numerically on the air/polymer and air/electrode interfaces with and without dielectric coating (represented by red and blue curves, respectively); (c) SEM images of the final structures corresponding to the bare upper electrode or dielectric-coated electrode; (d) SEM images of the mushroom-shaped microfiber arrays, which were obtained at voltages of 500, 600, and 700 V; (e) increasing tip diameter with the applied voltage at a capacitor clearance of 50 μm.

numerical simulation, the material properties, including the surface tension and dynamic viscosity coefficient, depending on the temperature, are considered as constant to simplify the calculation. This simplification could be acceptable, because in the real experiment, the electrically induced polymer deformation process is mostly conducted at a stationary temperature (~170 °C). Therefore, by defining $\omega(3\eta/\sigma h^3\alpha^4)$ and q/α as the dimensionless growth coefficient and wavenumber (written as ω^* and q^*), respectively, their mapping relationship determined by eq 3 is shown in Figure 2a. Clearly, when the dimensionless wavenumber q^* is <1.0, the dimensionless growth coefficient ω^* becomes >0, indicating a tendency of the pillar to grow upward. Otherwise, the initial micropillars would disappear (becoming flattened) due to the surface tension, which would overwhelm the electrohydrodynamic modulation. Because ε_p and σ (polymer's properties) and q (periodicity of the micropillar array) are all constant (with values of 3.5, 0.035 N/m, and $2\pi/30$ μm^{-1}, respectively) and $E_{max}^3 - E_{min}^3$ depends on both the capacitor clearance (l) and applied voltage (U), q^* can be simplified as a function of two variables, i.e., $q^* = f(l,U)$. For example, Figure 2b shows the dependence of q^* on U when the capacitor clearance is 40, 50, and 60 μm, and the initial micropillar array has a periodicity of 30 μm, a pillar diameter of 15 μm, and a height of 22 μm. The intersection of each solid curve with the dotted line ($q^* = 1.0$) provides a threshold voltage above which the pillars can be driven upward electrohydrodynamically by overcoming the surface tension, leading to a final contact to the upper electrode for an extended aspect ratio.

As mentioned previously, the capacitor clearance determines the final height of the mushroom-shaped microfibers, thus defining their aspect ratio (i.e., the ratio of the final fiber height to the middle pillar diameter). Obviously, a large aspect ratio can be obtained by increasing the clearance (as shown in Figure

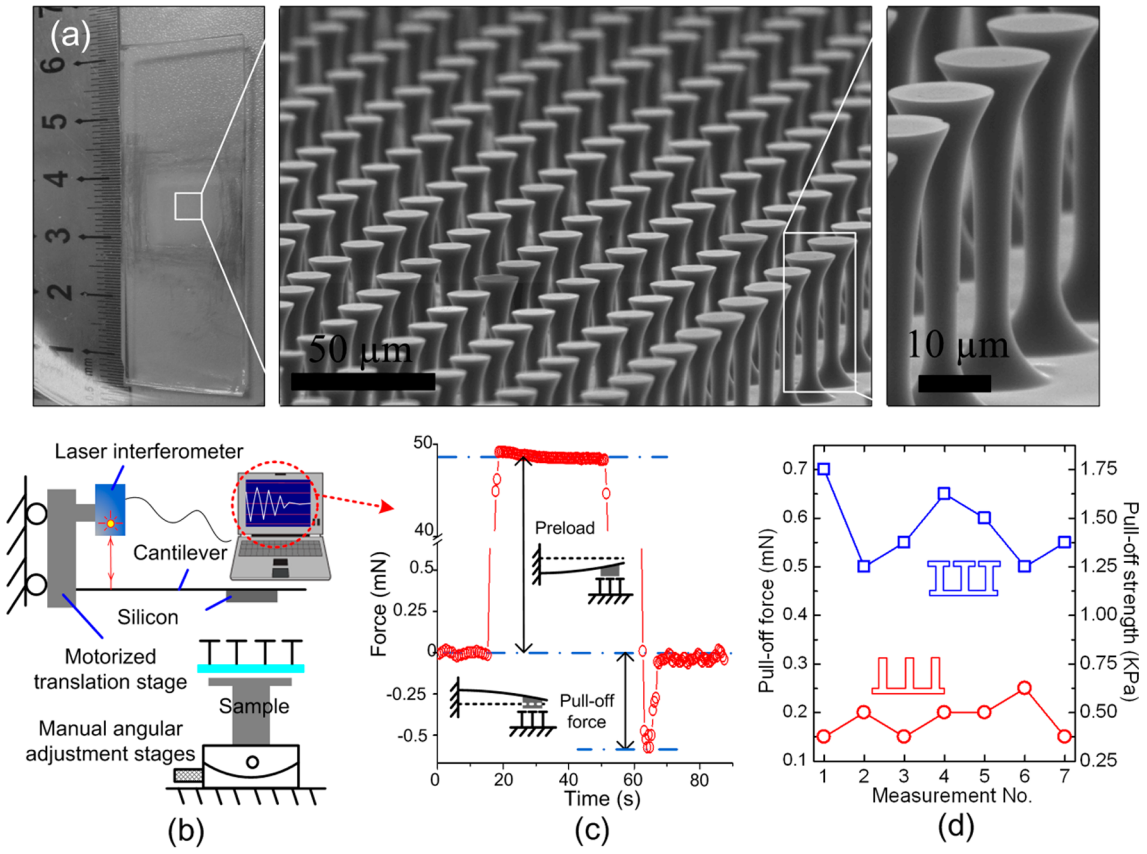

Figure 4. Testing of the dry adhesion of the samples fabricated by the EHD-based techniques: (a) photograph of a sample and SEM images of the corresponding microfiber array; (b) experimental setup for measuring dry adhesion; (c) force vs time according to a properly designed cantilever spring constant; (d) comparison of the adhesive force and strength between the mushroom-shaped microfiber array and the common microfiber array (with no mushroom tip endings). The preload for each measurement was ~70 mN.

2c), but correspondingly requires a high voltage for the initial growth of the preformed micropillars (as shown by the threshold voltage at the three different clearances in Figure 2b). The insets show the SEM images of the mushroom-shaped microfiber arrays obtained for the capacitor clearance of ~40, 50, and 60 μm, corresponding to voltages of 350, 550, and 750 V, respectively.

3.2. Electrowetting on the Upper Electrode for Large Microfiber Tips. In addition to the aspect ratio, a geometric parameter of the contact element (mushroom tip ending) of the microfibers such as the ratio of the tip diameter to the fiber diameter is also important in enhancing the adhesive performance.[36,37] It would be interesting to accomplish the fabrication of a high-aspect-ratio mushroom-shaped microfiber array simultaneously with controllable shapes for the tip ending in a convenient and cost-effective manner. In this study, through the EWOD effect, the diameter of the mushroom tips can be tuned by varying the applied voltage. Once the micropillars are electrohydrodynamically driven to contact the upper electrode, the subsequent transverse spreading of the polymer on the electrode can be considered as an electrowetting process of the polymer. To justify the importance of EWOD for the successful generation of mushroom-shaped microfibers with a large tip diameter, the effect of the dielectric SiO_2 layer on the electric field distribution was analyzed as follows.

EWOD has been widely known as an effective mechanism for manipulating liquid. As a general behavior of electrowetting, the air/polymer interface close to the electrode is driven outward (deformed from the pink line shape to the dark blue line shape in Figure 3a), and the dielectric layer increases the related driving force. Figure 3b shows the numerically computed results using the finite element method for the electric intensity distribution on the air/polymer and air/electrode interfaces with a bare electrode (the red curve) and a dielectric-coated electrode (the blue curve). The results show that the electric intensity at the air/polymer/electrode contact (an air/liquid/solid three-phase contact line) can be significantly enhanced due to the presence of a dielectric layer, and the correspondingly increased Maxwell force can be expected to drive the polymer into spreading transversely to an increased extent on the dielectric layer. Parts c(I) and c(II) of Figure 3 show the SEM images of the final microfiber arrays obtained without and with the dielectric layer, respectively, intuitively revealing the effectiveness of the EWOD for creating a large tip diameter for the biomimetic mushroom-shaped microfibers.

Because of the fact that the electrostatic force on a three-phase line is proportional to the applied voltage and is finally balanced by the air/polymer interfacial tension,[38] the tip diameter could be well controlled by fine-tuning the voltage above its critical value for a certain capacitor clearance as discussed previously. Figure 3d shows the SEM images of the mushroom-shaped microfiber arrays, with a tip ending diameter of ~11.3, 14.1, and 14.5 μm, corresponding to applied voltages of ~500, 600, and 700 V, respectively, for a capacitor clearance of 50 μm. Moreover, the tip ending diameter will tend to increase less significantly at a higher voltage, as shown in Figure 3e. This may be due to a saturation of the electrowetting effect

typical of EWOD. Notably, the transverse spreading of the upper part of a micropillar on the electrode corresponds to the shrinkage of its middle portion due to mass conservation, and the tip diameter should also be defined by taking the mechanical integrity of the shrinking microfiber shaft into account.

3.3. Testing of Dry Adhesion. To demonstrate a proof-of-concept of dry adhesion, a sample surface arrayed with the biomimetic mushroom-shaped microfibers was fabricated using the proposed approach, as shown in Figure 4a. The sample has a microfiber-arrayed area of ~1 cm^2, and the periodically distributed microfibers have a final fiber height of 47.8 μm and a middle diameter of 5.4 μm (i.e., an aspect ratio of ~9), a tip diameter of 14.4 μm, and a base diameter of 13.1 μm. An experimental setup was built in this study for adhesion measurement, as shown in Figure 4b. In this setup, cantilever deflections, which occurred at both the attachment and detachment of the sample to and from a 2 mm^2 Si wafer (glued on the cantilever) by moving the motorized translation stage (PI Gmbh M-531.DD with a resolution of 0.1 μm), were recorded using a laser interferometer (SIOS Messtechnik Gmbh SP-S with a resolution of 10 nm) and finally calibrated into force values.[39] The parallel alignment was guaranteed by the manual angular adjustment stages and two charge-coupled device (CCD) cameras. The cantilever used in the setup for the adhesive force measurement was made of stainless steel, which has a high Young's modulus of 200 GPa. The geometry of the cantilever was so designed (80 mm in length, 1 mm in width, and 0.5 mm in thickness) that an angular deflection of less than 0.05° was produced at its end even for the maximum adhesion detected in our experiment. Such a small deflection of the cantilever may justify the assumption that the planar probe and sample were in full contact during preloading and detaching before the adhesion failure occurred. Also, with this designed cantilever spring constant, the force measurement system was capable of a resolution of 0.05 mN. The force−time curve is shown in Figure 4c for a preload of 68.2 mN. The data points under 0 demonstrate a maximum adhesive force of 0.55 mN, which is actually the force experienced at the adhesion failure during the detachment process. Figure 4d shows the comparison of the adhesive force and strength between the ordinary (red points) and mushroom-shaped (blue points) microfiber arrays. The enhanced adhesive force for the latter is considered to result from the presence of the specific contact element (mushroom tip ending), which not only increased the contact area, but also improved the stress distribution in the interface at the detachment process.[4,8] Additionally, as a result of the limited resolution of the measurement setup, the adhesive force of a flat (not patterned) reference sample cannot be detected. In other words, the adhesive force of the flat sample is less than the resolution of the setup, 0.05 mN. These results prove that the contact splitting generated by the microfiber arrays (ordinary column or mushroom shape) would result in a much higher adhesive force compared to that of the flat surface.[4−6,30,31] However, the adhesive force of the PMMA mushroom-shaped microfiber array is lower compared to that of the gecko system and typical gecko-inspired adhesive.[4,6−8] This can be largely attributed to the terribly nonadhesive material used in this experiment, resulting in a relatively poor compliance with the target surface on a microscopic scale. To increase the adhesion of the mushroom-shaped PMMA microfibers, a thin film of a sticky material can be created on the microfibers by a deposition or coating process which has to be explored.

4. CONCLUSION

In this paper we report a three-step process for producing mushroom-shaped microfibers with a well-controlled aspect ratio and tip diameter, suitable potentially for almost any thermoplastic polymers (including various mechanically strong or hard polymers such as PMMA used in this experiment). Hot embossing was used to generate an initial micropillar array with a low aspect ratio, which was then electrohydrodynamically pulled to contact the upper plate. The electrowetting of the preformed micropillar array on the upper electrode surface produced a microfiber array with a tip diameter which was dependent on the applied voltage and electrowetting. Electrowetting on a dielectric (enabled by coating a dielectric SiO_2 layer in this experiment) proved to be effective for increasing the tip diameter of the microfibers. The experiment on dry adhesion of a surface with such a biomimetic structure successfully demonstrated the applicability of the proposed idea.

AUTHOR INFORMATION

Corresponding Author

*E-mail: jyshao@mail.xjtu.edu.cn.

Notes

The authors declare no competing financial interest.

ACKNOWLEDGMENTS

This work was financed by the National Natural Science Foundation of China (NSFC) Major Research Plan on Nanomanufacturing (Grant 91323303), NSFC Fund (Grants 51175417 and 51305347), and Program for New Century Excellent Talents in University (Grant NCET-13-0454).

REFERENCES

(1) Autumn, K.; Liang, Y. A.; Hsieh, S. T.; Zesch, W.; Chan, W. P.; Kenny, T. W.; Fearing, R.; Full, R. J. Adhesive Force of a Single Gecko Foot-Hair. *Nature* **2000**, *405*, 681−685.

(2) Jeong, H. E.; Suh, K. Y. Nanohairs and Nanotubes: Efficient Structural Elements for Gecko-Inspired Artificial Dry Adhesives. *Nano Today* **2009**, *4*, 335−346.

(3) Tian, Y.; Pesika, N.; Zeng, H. B.; Rosenberg, K.; Zhao, B. X.; McGuiggan, P.; Autumn, K.; Israelachvili, J. Adhesion and Friction in Gecko Toe Attachment and Detachment. *Proc. Natl. Acad. Sci. U.S.A.* **2006**, *103*, 19320−19325.

(4) Gorb, S.; Varenberg, M.; Peressadko, A.; Tuma, J. Biomimetic Mushroom-Shaped Fibrillar Adhesive Microstructure. *J. R. Soc., Interface* **2007**, *4*, 271−275.

(5) Arzt, E.; Gorb, S.; Sphlenak, R. From Micro to Nano Contacts in Biological Attachment Devices. *Proc. Natl. Acad. Sci. U.S.A.* **2003**, *100*, 10603−10606.

(6) Murphy, M. P.; Kim, S.; Sitti, M. Enhanced Adhesion by Gecko-Inspired Hierarchical Fibrillar Adhesives. *ACS Appl. Mater. Interfaces* **2009**, *1*, 849−855.

(7) Wang, Y.; Hu, H.; Shao, J. Y.; Ding, Y. C. Fabrication of Well-Defined Mushroom-Shaped Structures for Biomimetic Dry Adhesive by Conventional Photolithography and Molding. *ACS Appl. Mater. Interfaces* **2014**, *6*, 2213−2218.

(8) Carbone, G.; Pierro, E.; Gorb, S. N. Origin of the Superior Adhesive Performance of Mushroom-Shaped Microstructured Surfaces. *Soft Matter* **2011**, *7*, 5545−5552.

(9) Del Campo, A.; Greiner, C.; Arzt, E. Contact Shape Controls Adhesion of Bioinspired Fibrillar Surfaces. *Langmuir* **2007**, *23*, 10235−10243.

(10) Del Campo, A.; Greiner, C.; Alvarea, I.; Arzt, E. Patterned Surfaces with Pillars with Controlled 3D Tip Geometry Mimicking Bioattachment Devices. *Adv. Mater.* **2007**, *19*, 1973−1977.
(11) Jeong, H. E.; Lee, J. K.; Kim, H. N.; Moon, S. H.; Suh, K. Y. A Nontransferring Dry Adhesive with Hierarchical Polymer Nanohairs. *Proc. Natl. Acad. Sci. U.S.A.* **2009**, *106*, 5639−5644.
(12) Zhou, M.; Tian, Y.; Sameoto, D.; Zhang, X. J.; Meng, Y. G.; Wen, S. Z. Controllable Interfacial Adhesion Applied to Transfer Light and Fragile Objects by Using Gecko Inspired Mushroom-Shaped Pillar Surface. *ACS Appl. Mater. Interfaces* **2013**, *5*, 10137−10144.
(13) Heepe, L.; E. Kovalev, A.; Filippov, A. E.; Gorb, S. N. Adhesion Failure at 180000 Frames per Second: Direct Observation of the Detachment Process of a Mushroom-Shaped adhesive. *Phys. Rev. Lett.* **2013**, *111*, 104301−104305.
(14) Davies, J.; Hag, S.; Hawke, T.; Sargent, J. P. A Practical Approach to the Development of a Synthetic Gecko Tape. *Int. J. Adhes. Adhes.* **2009**, *29*, 380−390.
(15) Sameoto, D.; Menon, C.; Deep, U. V. Patterning of Acrylic Masters for Molding Biomimetic Dry Adhesives. *J. Micromech. Microeng.* **2010**, *20*, 115037−115046.
(16) Sameoto, D.; Menon, C. A Low-Cost, High-Yield Fabrication Method for Producing Optimized Biomimetic Dry Adhesives. *J. Micromech. Microeng.* **2009**, *19*, 115002−115008.
(17) Song, J.; Mengüc, Y.; Sitti, M. Enhanced Fabrication and Characterization of Gecko-Inspired Mushroom-Tipped Microfiber Adhesives. *J. Adhes. Sci. Technol.* **2013**, *27*, 1921−1932.
(18) Kim, S.; Sitti, M. Biologically Inspired Polymer Microfibers with Spatulate Tips as Repeatable Fibrillar Adhesives. *Appl. Phys. Lett.* **2006**, *89*, 261911−261913.
(19) Kim, S.; Aksak, B.; Sitti, M. Enhanced Friction of Elastomer Microfiber Adhesives with Spatulate Tips. *Appl. Phys. Lett.* **2007**, *91*, 221913−221915.
(20) Rohrig, M.; Thiel, M.; Worgull, M.; Holscher, H. 3D Direct Laser Writing of Nano- and Microstructured Hierarchical Gecko-Mimicking Surfaces. *Small* **2012**, *8*, 3009−3015.
(21) Jeong, H. E.; Suh, K. Y. Precise Tip Shape Transformation of Nanopillars for Enhanced Dry Adhesion Strength. *Soft Matter* **2012**, *8*, 5375−5380.
(22) Murphy, M. P.; Aksak, B.; Sitti, M. Gecko-Inspired Directional and Controllable Adhesion. *Small* **2009**, *5*, 170−175.
(23) Tian, H. M.; Shao, J. Y.; Ding, Y. C.; Li, X. M.; Hu, H. Electrohydrodynamic Micro-/Nanostructuring Processes Based on Prepatterned Polymer and Prepatterned Template. *Macromolecules* **2014**, *47*, 1433−1438.
(24) Li, X. M.; Shao, J. Y.; Tian, H. M.; Ding, Y. C.; Li, X. M. Fabrication of High-Aspect-Ratio Microstructures Using Dielectrophoresis-Electrocapillary Force-Driven UV-Imprinting. *J. Micromech. Microeng.* **2011**, *21*, 065010−065019.
(25) Kwak, M. K.; Pang, C.; Jeong, H. E.; Kim, H. N.; Yoon, H.; Jung, H. S.; Suh, K. Y. Towards the Next Level of Bioinspired Dry Adhesives: New Designs and Applications. *Adv. Funct. Mater.* **2011**, *21*, 3606−3616.
(26) Tian, H. M.; Shao, J. Y.; Ding, Y. C.; Li, X.; Li, X. M. Numerical Studies of Electrically Induced Pattern Formation by Coupling Liquid Dielectrophoresis and Two-Phase Flow. *Electrophoresis* **2011**, *32*, 2245−2252.
(27) Tian, H. M.; Shao, J. Y.; Ding, Y. C.; Li, X. M.; Liu, H. Z. Numerical Characterization of Electrohydrodynamic Micro- or Nanopatterning Processes Based on a Phase-Field Formulation of Liquid Dielectrophoresis. *Langmuir* **2013**, *29*, 4703−4714.
(28) Pollack, M. G.; Fair, R. B.; Shenderov, A. D. Electrowetting-Based Actuation of Liquid Droplets for Microfluidic Applications. *Appl. Phys. Lett.* **2000**, *77*, 1725−1726.
(29) Jones, T. B. On the Relationship of Dielectrophoresis and Electrowetting. *Langmuir* **2002**, *18*, 4437−4443.
(30) Persson, B. N. J. On the Mechanism of Adhesion in Biological Systems. *J. Chem. Phys.* **2003**, *118*, 7614−7621.
(31) Autumn, K.; Majidi, C.; Groff, R. E.; Dittmore, A.; Fearing, R. Effective Elastic Modulus of Isolated Gecko Setal Arrays. *J. Exp. Biol.* **2006**, *209*, 3558−3568.
(32) Schaffer, E.; Thurn-Albrecht, T.; Russell, T. P.; Steiner, U. Electrically Induced Structure Formation and Pattern Transfer. *Nature* **2000**, *403*, 874−877.
(33) Arun, N.; Sharma, A.; Pattader, P. S. G.; Banerjee, I.; Dixit, H. M.; Narayan, K. S. Electric-Field-Induced Patterns in Soft Viscoelastic Films: From Long Waves of Viscous Liquids to Short Waves of Elastic Solids. *Phys. Rev. Lett.* **2009**, *102*, 254502−254505.
(34) Goldberg-Oppenheimer, P.; Steiner, U. Rapid Electrohydrodynamic Lithography Using Low-Viscosity Polymers. *Small* **2010**, *6*, 1248−1254.
(35) Tian, H. M.; Ding, Y. C.; Shao, J. Y.; Li, X. M.; Liu, H. Z. Formation of Irregular Micro- or Nano-Structure with Features of Varying Size by Spatial Fine-Modulation of Electric Field. *Soft Matter* **2013**, *9*, 8033−8040.
(36) Carbone, G.; Pierro, E. Sticky Bio-inspired Micropillars: Finding the Best Shape. *Small* **2012**, *8*, 1449−1454.
(37) Aksak, B.; Sahin, K.; Sitti, M. The Optimal Shape of Elastomer Mushroom-Like Fibers for High and Robust Adhesion. *Beilstein J. Nanotechnol.* **2014**, *5*, 630−638.
(38) Li, X. M.; Ding, Y. C.; Shao, J. Y.; Tian, H. M.; Liu, H. Z. Fabrication of Microlens Arrays with Well-Controlled Curvature by Liquid Trapping and Electrohydrodynamic Deformation in Microholes. *Adv. Opt. Mater.* **2012**, *24*, 165−169.
(39) Kustandi, T. S.; Samper, V. D.; Yi, D. K.; Ng, W. S.; Neuzil, P.; Sun, W. Self-Assembled Nanoparticles Based Fabrication of Gecko Foot-Hair-Inspired Polymer Nanofibers. *Adv. Funct. Mater.* **2007**, *17*, 2211−2218.